

AD-A133 900

THE GASEOUS AND PLASMA ENVIRONMENT AROUND SPACE SHUTTLE 1/1
(U) AIR FORCE GEOPHYSICS LAB HANSCOM AFB MA
R NARCISI ET AL. 13 OCT 83 AFGL-TR-83-0261

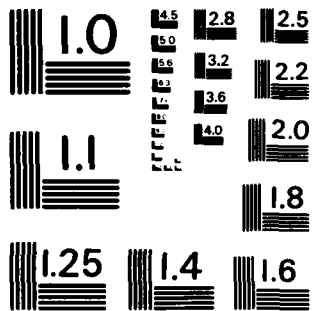
UNCLASSIFIED

F/G 22/2

NL



END
DATE
FILMED
*1
DTIC



MICROCOPY RESOLUTION TEST CHART
NATIONAL BUREAU OF STANDARDS-1963-A

pointed in the ram direction.⁸ The spectrometer is fixed on 16 amu (O^+) for 32 steps and then 30 amu (NO^+) for 32 steps. For O^+ , the V_r grid is stepped from -4.45 volts to +7.91 volts and for NO^+ , from -6.05 to +12.50 volts. This mode makes use of the fact that the shuttle velocity is constant at about 8 kilometers per second so that the energy in electron volts of the incoming ions is equal to one third the mass number in AMU. Therefore, for a zero volt shuttle potential, the O^+ current should start to decrease in magnitude at $V_r = +5.33$ volts and for NO^+ at +10 volts.

The neutral mode consists of two groups of 64 measurements. The first group measures masses between 1 and 67 amu plus two steps for total ions greater than 50 amu, all in the non-retarded (NR) mode. The same measurements are made for the second group of 64 but with a retarding potential of 2.5 volts on the V_r grid. As in the positive ion mode for ram conditions, the difference between the retarded and non-retarded measurements identifies the contaminant species.

For all operating modes, the ion current to a sampling grid is measured before the ions enter the quadrupole filter. The measured grid currents relate to the ambient ion densities in the ion mode and to the ion source pressure in the neutral mode which, in turn, can be used to determine ambient and contaminant densities. Contaminant neutral species concentrations are much more difficult to obtain and require the use of complex scattering programs like SPACE 2 to interpret the measurements. The spatial resolution of the grid current measurements is 80 meters; however, it is only limited by the sampling rate available on shuttle.

The instrument was mounted such that it was looking horizontally over the right wing but pitched upward 12° from the right wing or y-axis. The instrument's field of view was a 20° cone for ions and about 2π for neutrals.

Data Acquisition Program

Over the entire period of the Space Shuttle's flight the instrument was commanded on 158 times with data gathering periods varying from as short as 5 minutes to as long as 45 minutes over orbits spanning from Rev. 3.6 to 94.9. There were four data gathering programs: 1) all ion; 2) all neutral; 3) 5 min. neutral - 5 min. ion; and 4) 5 min. neutral - 5 min. ion - the remainder neutral. The measurements were further programmed around engine firings, water dumps, studies of ionospheric irregularities, and other events. The vacuum cap was opened on orbit 3.0 and closed on orbit 94.9 sealing the instrument.

Neutral Pressure and Ion Density Conversion Factors

The measurements are presented in terms of measured currents versus Mission Elapsed Time (MET) in seconds. For the neutral mode, species pressures and densities have not yet been calculated because the spacecraft attitude data are not finalized. Figure 1 gives a grid current-to-ion source pressure conversion curve for nitrogen (N_2) gas which generally can be used to obtain a rough estimate of internal (ion source) pressures. (The gas composition must be taken into account for an accurate pressure determination.) For the ion mode, the grid current

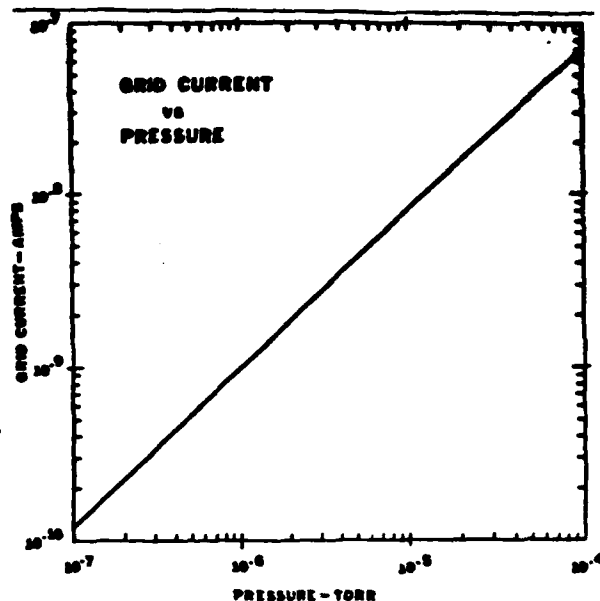


Fig. 1 Ion source pressure versus measured grid current for nitrogen (N_2).

(Density Monitor) can be multiplied by 2×10^{13} ions cm^{-3} amp^{-1} to obtain total ion density to within a factor of two for ram conditions. Normalization to other plasma density measurements on the spacecraft will increase the accuracy of this factor. The output of the ion species may then be scaled to the total number density to obtain species concentrations.

Neutral Mode Measurements

Thruster Firing Effects

Engine firings produce significant perturbations of light, particles and gases. With up to 40,000 engine burns over a typical flight, a significant disturbance occurs about once every 15 seconds on average, each with varying duration. To circumvent this problem, various experimenters have obviously requested the engines be inactivated during their measurements. The mass spectrometer has the capability to characterize the exhaust gas products and their return fluxes.

Figures 2 and 3 present sample measurements from orbit 4.6 taken at night near -27° latitude with the instrument's angle of attack at 90° and the shuttle flying in an airplane mode. The interesting features of orbit 4.6 are the measured gas return fluxes from the vernier and OMS-4 burns. For all three cases, the pressure pulses are about 10^{-6} torr, and in a matter of 1-2 seconds after engine shut down, all levels are back to normal (see Figure 4). The three major engine exhaust products are H_2 , H_2O and N_2 with relative concentrations of 0.6, 0.3 and 0.1, respectively for the OMS-4 burn. For the first vernier pressure pulse, the relative concentrations are 0.11, 0.51 and 0.38 and for the second 0.11, 0.36 and 0.53, respectively. There do not appear to be any significant amounts of CO or CO_2 in the return flux. Disregarding the absence of CO and CO_2 , the expected and measured relative composition of the vernier exhaust products compare fairly well, while the OMS flux is clearly rich in H_2 . This behavior may be due to the larger molecular scattering efficiency of H_2 which

Backscattered Energetic Particles

An interesting event occurred in orbit 5.4, apparently the directed flux of ambient species imparted some energy to the shuttle contaminants through elastic collisions. Figure 5 presents the measured H₂O and He contaminants showing a broad, bell-shaped pressure enhancement with a maximum increase of a factor of 2.5 while H₂O exhibits a factor of about 7 increase. In sharp contrast, He mirrors the H₂O behavior. Both the retard and non-retard H₂O and He measurements are presented in Figure 14. It is noted that the retard current rises dramatically and is almost equivalent to the non-retard current at the H₂O peak. This pattern does not occur for He and implies that a significant percentage of the incoming H₂O flux had energies in excess of 2.5 eV. The only known way this could happen is through elastic collisions with ambient species. Perhaps, also, the ambient flux is grazing the densest portion of the outgassing layer to produce a large backscattered flux. The decrease in He may occur if the principal source region was downstream from the mass spectrom-

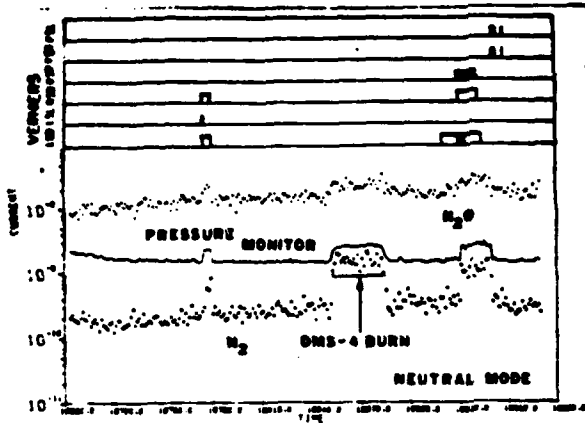


Fig. 2 Orbit 4.6 measurements of N₂, H₂O and the pressure monitor exhibiting the effects of the Vernier and OMS burns.

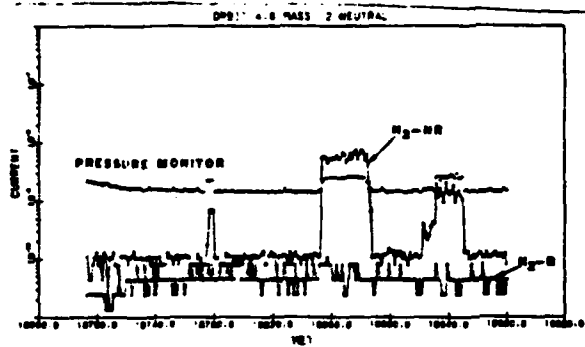


Fig. 3 Orbit 4.6 measurements of hydrogen showing clear increases due to the engine firings.

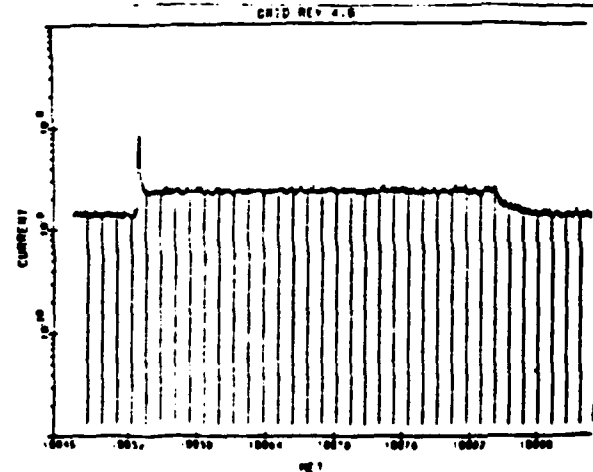


Fig. 4 Pressure monitor output for orbit 4.6 at the full 100 samples per second data rate showing the OMS-4 burn. Disregard vertical lines in the current output.

must be scattered forward from a plume directed to the rear of the spacecraft. In the case of the verniers, the return flux is detected mainly from the verniers located on the spectrometer's pointing side.

ORBIT 5.4 MASS 4 NEUTRAL

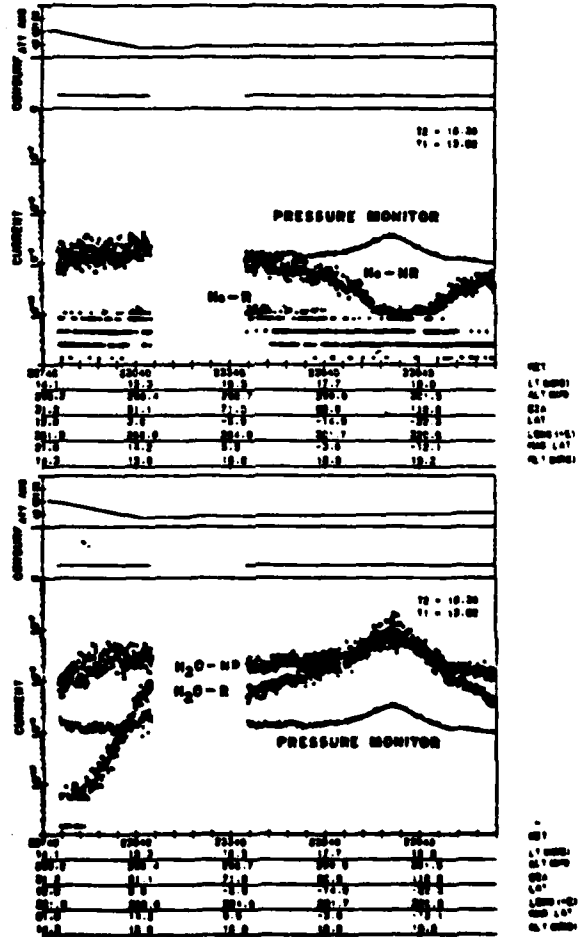


Fig. 5 Water vapor and helium contaminants measured on orbit 5.4 demonstrating the helium mirror image of the pressure bulge and the increase of H₂O currents in the retard mode.

eter, such that the He can be "washed" away from the mass spectrometer. From 23,340 seconds MET until the end of the measurements there were no engine firings, no water dumps and basically nothing to explain this behavior. The only variable was the instrument attack angle which smoothly and slowly increased monotonically by only 5°. Other species like the TI measurements for ions greater than 50 amu show a response similar to He while mass 16 (O) is similar to the H₂O behavior. More study is required of the complex collisional scattering processes to explain these measurements.

Measurements During Water Dumps

A supply water dump of 124 lbs at an average dump rate of 158 lb/hr occurred between 28,920 and 31,740 seconds MET. Within this same time period, a waste water dump of 85 lbs at a dump rate of 150 lb/hr took place between 29,160 and 31,200 seconds MET. Neutral mode measurements were made after the start of the water dumps between 29,620 and 29,860 seconds on orbit 6.7. The H₂O and pressure monitor outputs for orbit 6.7 are shown in Figure 6 along with a plot of the VCS firings. The instrument's attitude or attack angle is about 105° (toward wake). The water vapor output increased by about a factor of 8 from the beginning to the end of the run and may be associated with the water dump. The relatively flat

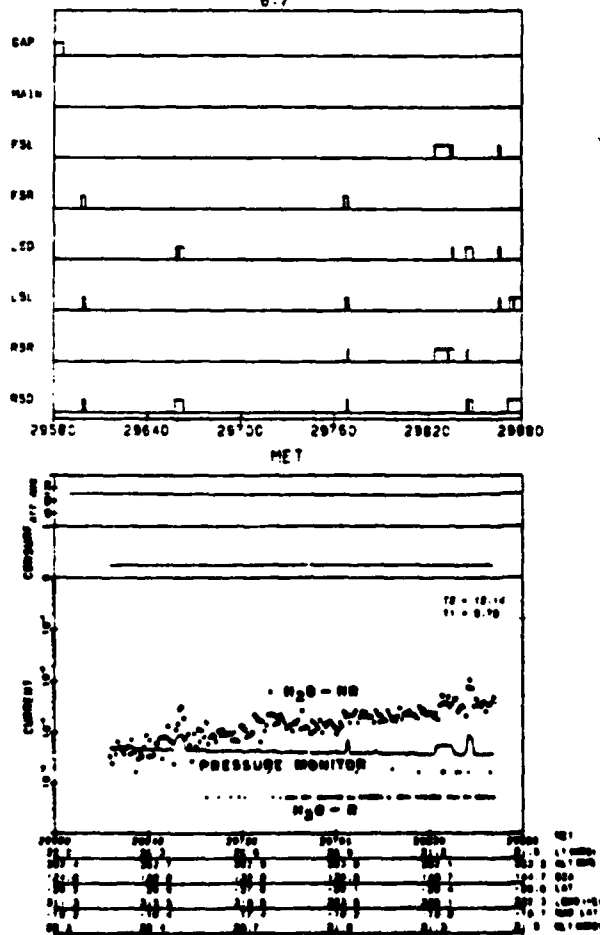


Fig. 6 Water vapor measurements during water dumps and VCS firings.

pressure monitor does not reflect the H₂O rise, because other species at 4, 28, 30, 32 and 44 amu were more flat and dominating. Four distinct increases are seen on the pressure monitor, and these are all directly associated with VCS firings.

Average Flight Behavior of Neutral Species

To determine possible trends in the neutral species throughout flight, the several hundred or so mass peak currents over a particular run were simply averaged to one point and plotted versus a mean MET. Flight perturbation events, instrument angle of attack and in fact, all other parameters or corrections were completely disregarded. Rather than show all the species we shall concentrate on shuttle contaminants and the ion source pressure excursions. The two dominant contaminants were H₂O and He. Whereas H₂O can cause both instrumental degradation as well as measurement perturbations, especially in the infrared, He is rather benign. Figure 7 presents the plot of the average H₂O behavior throughout flight with superimposed spectrometer sensor temperature measurements. The correlation between the H₂O and temperature profiles is remarkable. The more than two orders of magnitude variation in the H₂O output certainly cannot be caused by the sensor outgassing over the temperature range of only about 5-25°C.

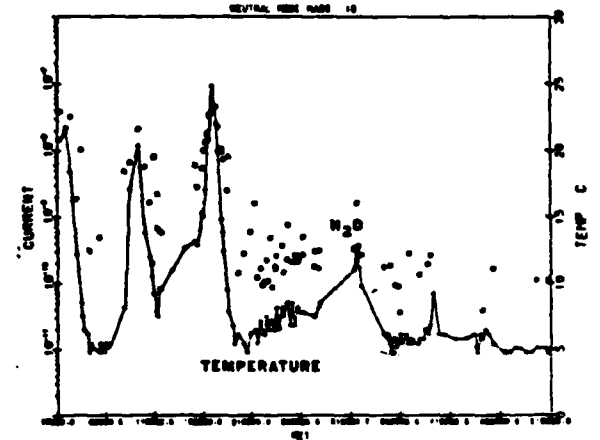


Fig. 7 The average H₂O currents and sensor temperature measurements throughout flight. Note the striking similarity in these two parameters.

The sensor, however, had an active temperature controller while thermistors placed throughout the pallet, although showing identical profiles, had temperature excursions to at least 100°C at the peaks. Thus, it is probable that the H₂O output is directly reflecting the temperature-induced outgassing of spacecraft surfaces. In the neutral mode the instrument has almost a 2x field of view and thus can accept a direct outgassing flux from substantial surface area in front of the instrument as well as the backscattered flux from the ambient. A determination of these fluxes is being attempted using the SPACE 2 computer code. It is, therefore, difficult at the present time to determine the water vapor concentrations near the shuttle from the neutral mode measurements. In fact, as discussed below under the ion mode measurements, it may turn out to be easier using the plasma measurements of O⁺, H₂O⁺ and H₃O⁺ and the associated ion-molecule reactions to calculate H₂O concentrations. Never-

theless, the spacecraft temperatures, which vary considerably throughout the shuttle, seem to be a significant controlling factor to the water vapor environment. Although requiring future confirmation, it appears that the early time H_2O concentrations and those near the two peaks between 60,000 and 210,000 seconds may prove to be deleterious to certain IR measurements.

Helium is also a significant contaminant over the whole flight as seen in Figure 8. For the most part, the helium currents span the range from 10^{-10} to 6×10^{-9} amps or roughly 4×10^{-9} to 2.3×10^{-7} torr. The maximum ambient He ram pressure is about 6×10^{-9} torr or 1.5×10^{-10} amps, so that most of the He is due to shuttle, especially since most of the measurements were not made in ram. To achieve He pressures up to 2×10^{-7} torr in the spectrometer requires a very high helium leak rate.

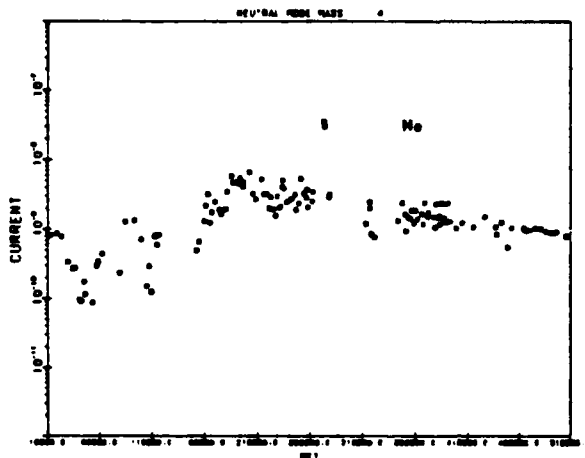


Fig. 8 Average helium currents over the seven day flight.

Average currents for the total ions (TI) greater than 50 amu measurements are shown in Figure 9. The current range is about 1×10^{-10} to 2×10^{-9} amps. There are indications of increases at the temperature peaks. The TI mode is about 40 times more sensitive than the mass scan mode. Although dependent upon the ionization cross sections for the heavy masses, a TI>50 amu gas pressure of less than 10^{-9}

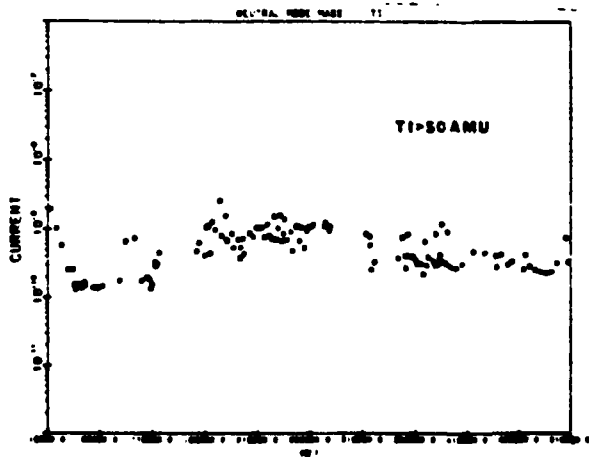


Fig. 9 Current averages for TI >50 amu throughout the flight.

torr is estimated. Further, some of the TI signal may result from ion source outgassing. All this information points to very low gas concentrations for the heavy masses.

Figure 10 presents the average grid currents. Using the calibration curve in Figure 1, the average ion source pressures are generally between 10^{-7} to 7.5×10^{-6} torr with a downward trend with time. The ion source never attained ambient pressures ($\sim 6 \times 10^{-8}$ torr) even in wake sampling attitudes. This is not surprising since it takes about a week or so for "clean" satellites to fully degas. Much of the data was taken in non-ram (high attack angle) conditions so that a significant portion of these pressures was due to outgassing species.

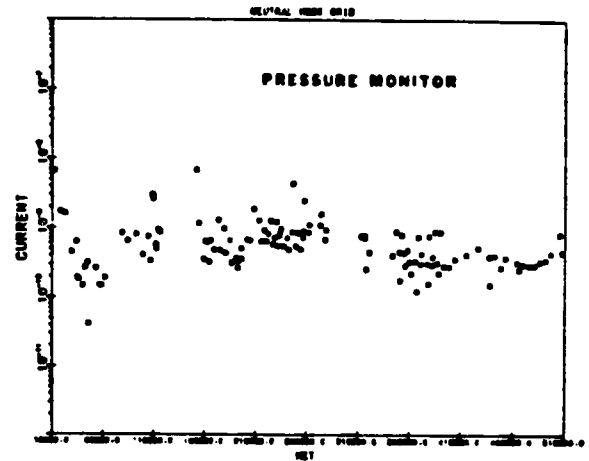


Fig. 10 Average neutral mode grid currents throughout flight.

Ion Mode Measurements

Contamination and Thruster Firing Effects

Figure 11 shows daytime measurements at 298.5 km of O^+ , N^+ , H_2O^+ and the density monitor for orbit 5.4. The O^+ output is depressed because the instrument's attack angle was high, varying from 33° to 38° while the instrument's unimpeded field of view is a 20° cone. The H_2O^+ ions are produced from the rapid charge transfer reaction, $O^+ + H_2O \rightarrow H_2O^+ + O$. For ram conditions in orbit 3.6 (not shown), the H_2O^+/O^+ ratio was about 10%. In orbit 5.4 this ratio was unity and greater and the H_2O^+ currents are 10x larger than the 3.6 orbit values probably due to the 10x greater daytime O^+ concentrations. The H_2O^+ output does not exhibit a strong dependence on the attack angle, perhaps because the H_2O^+ ions have a thermal distribution since there is essentially no momentum transfer in the above reaction. In Figure 11, the H_2O^+ currents are about equal to and then exceed the O^+ currents as the angle of attack becomes larger. Figure 12 shows the same orbit 5.4 measurements but compares the N_2O^+ and H_2O^+ outputs. The H_2O^+ ions are produced from the $H_2O^+ + H_2O \rightarrow H_3O^+ + OH$ fast reaction. The H_3O^+ currents also rise with increasing attack angle and their relatively large concentrations are indicative of significant H_2O pressures around the spacecraft. We are in the process of using these measurements and the ion-molecule reactions to deduce neutral H_2O concentrations.

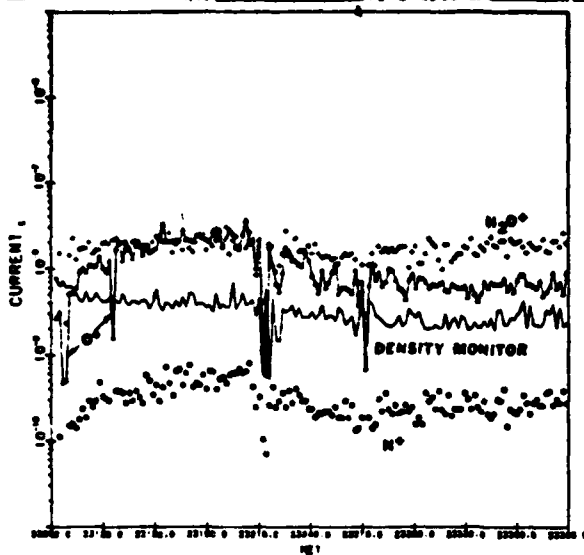


Fig. 11 Orbit 5.4 daytime measurements of O^+ , N^+ , H_2O^+ and the density monitor. The instrument's attack angle varied from 33° to 38° .

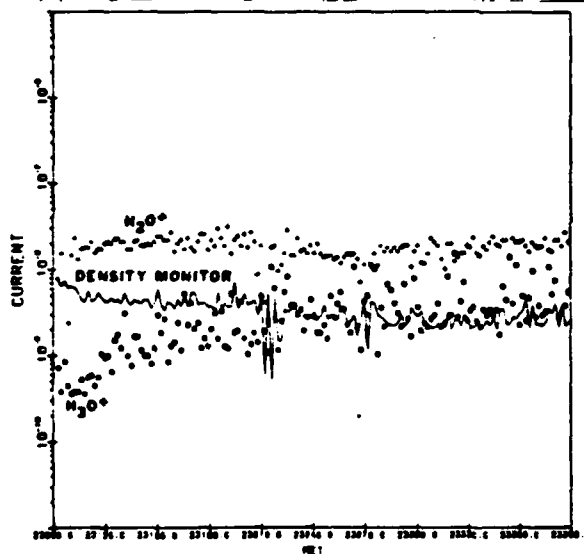


Fig. 12 Orbit 5.4 measurements similar to Figure 11, comparing the H_2O^+ and H_3O^+ outputs along with the density monitor.

These measurements in Figures 11 and 12 demonstrate not only the effects of water vapor contamination but also of thruster burns. The several depletions in the vicinity of 23,210 and 23,270 seconds MET are due to VCS firings. The density monitor shows plasma depletions as large as a factor of ten, as also reflected by the O^+ and N^+ outputs.

Although not shown here, reactions with the exhaust gases were also measured. Specifically, there were N_2^+ , NO^+ and OH^+ enhancements produced by $O^+ + N_2 \rightarrow N_2^+ + O$, $O^+ + N_2 \rightarrow NO^+ + N$ and $O^+ + N_2 \rightarrow OH^+ + N$. On the other hand H_2O^+ showed a depletion, mainly because the neutral H_2O concentrations were already large (comparable to the engine exhaust H_2O), and,

in addition, there was a diminished production of H_2O^+ ions due to the depleted O^+ ions. Most of the data has not yet been examined to determine the total number of thruster firing measurements; however, another example is shown in Figure 13 for orbit 49.7. This particular run was chosen because it also demonstrates the much stronger angle of attack dependence of the mass spectrometer output on O^+ than on the density monitor output.

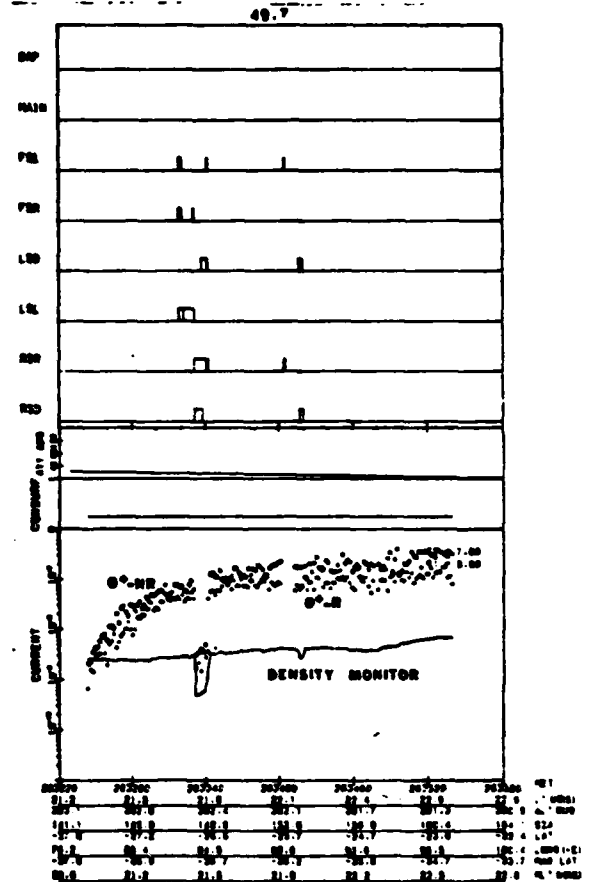


Fig. 13 Orbit 49.7 measurements of O^+ and the density monitor demonstrating the angle of attack dependence on the outputs as well as thruster firing effects.

Equatorial Ionospheric Irregularities

The equatorial orbit of shuttle allowed for measurements of equatorial spread F. The ionospheric E region collapses after sunset, and an F region ledge with an unstable sharp gradient is formed. Plasma depletions are generated within the ledge which then rise, forming instabilities from the base of the F region up to ~ 1000 km. These "plumes" or "bubbles" are often seen between sunset and sunrise at equatorial latitudes and can cause up to 30% outages of UHF transmissions. Measurements of equatorial irregularities at 301 ± 1 km were obtained on a 42.5 minute nighttime portion of orbit 24.6. The instrument was in the ram position for the entire pass. Figure 14 shows the O^+ , N^+ and density monitor outputs for orbit 24.6. The total ion density averages about 3×10^3 ions cm^{-3} before the depletions. The greatest depletion is about 10^4 ions

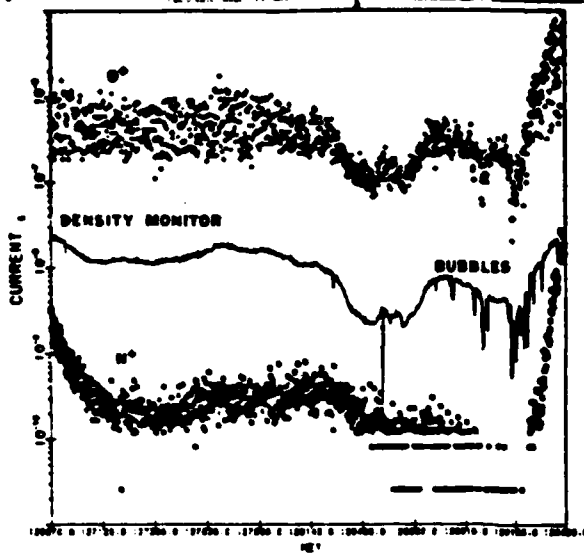


Fig. 14 Orbit 24.6 measurements of O^+ , N^+ and the density monitor showing regions of ionospheric irregularities near the equator.

cm^{-3} or a factor of 30 down from ambient. Only one sample per second of the density monitor's 100 sample per second output is plotted in Figure 14. It is, therefore, possible in the future to expand the region of the depletions for higher spatial resolution and to obtain density power fluctuation spectra by FFT. We have no explanation at this time for the large fluctuations in the O^+ signals, since the density monitor is relatively smooth. The rise in density at the end of the run is due to sunrise.

Figure 15 shows the same orbit 24.6 measurements except that the H_2O^+ output replaces the N^+ output. The H_2O^+/O^+ ratio is about 2% and is fairly constant over the 42.5 minute run implying a constant H_2O concentration over this period. The H_2O^+/O^+ ratio was about 10% on orbit 3.6; therefore, the H_2O concentration was about a factor of 5 less for orbit 24.6 since this ratio should be directly proportional to the H_2O concentration.

Vehicle Potential Measurements

Figure 16 presents samples of the vehicle potential mode of operation from orbit 3.6. The drop-off in current for O^+ occurs at approximately 6.3 volts indicating a vehicle potential of about -1 volt since the energy of O^+ ions with zero vehicle potential would be 5.33 electron volts. Fall-off for NO^+ occurs at about 11 volts also indicating a vehicle potential of about -1 volt since the NO^+ energy is 10 electron volts. Most of the vehicle potential mode data has not yet been reduced so that it is not currently possible to determine the variations of spacecraft potential with time.

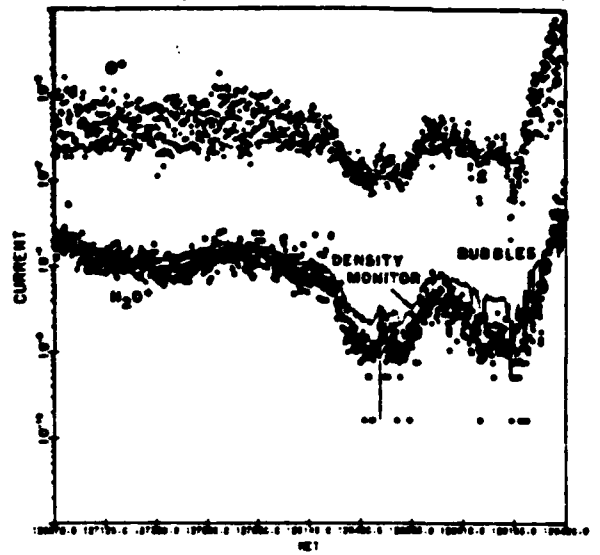


Fig. 15 Similar to Figure 14 but replacing the N^+ output with the H_2O^+ measurements.

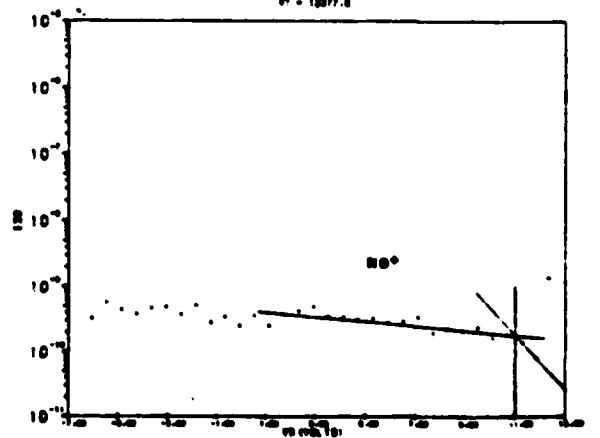
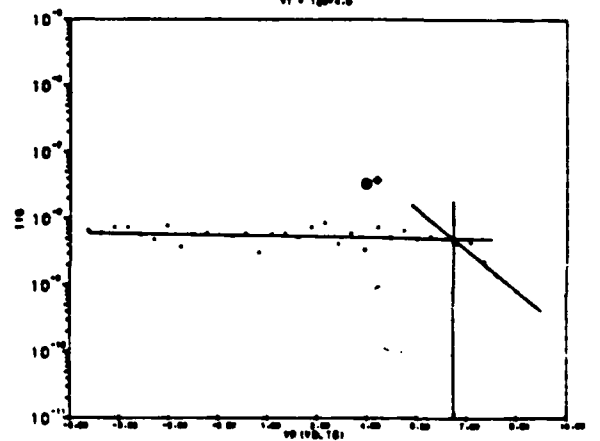


Fig. 16 Examples of vehicle potential measurements for orbit 3.6.

Conclusions

The mass spectrometer measurements have provided a wealth of information. A preliminary examination of just some of the data led to the following observations:

(a) The largest important contaminant was water vapor and, except for thruster burns and water dumps, its quantity seems to be directly controlled by the temperature of spacecraft surfaces.

(b) Helium was a major contaminant throughout flight with concentrations approaching those of H₂O.

(c) The return gas flux due to OMS and VCS burns produced pressure pulses of $1-2 \times 10^{-6}$ torr rising immediately with engine initiation and falling to background levels within a few seconds of engine cut-off. The major engine exhaust products were H₂, H₂O and H₂. The return flux was greatest from the verniers on the spectrometer pointing side.

(d) Species with masses larger than 50 amu were always in small concentrations.

(e) Measurements of energetic backscattered neutral molecules were made and will aid in understanding the complex scattering processes.

(f) Neutral measurements during water dumps showed a steadily rising H₂O signal.

(g) Plasma depletions, typically as large as a factor of about 10, were observed during thruster firings. Enhancements of N₂⁺, NO⁺ and OH⁺ were measured during the firings. These ion species were created by ion molecule reactions between O⁺ and the exhaust gases.

(h) It is possible to determine both the change and, in the future, concentrations of H₂O near the vehicle from the plasma measurements of the H₂O⁺/O⁺ ratio and from measurements of H₃O⁺ also.

(i) Despite the contamination, it was still possible to measure accurately ionospheric irregularities and the ambient plasma while in the ram sampling configuration, since the contaminant disturbances were small.

(j) It was demonstrated that vehicle potential measurements can be performed using the spectrometer.

In conclusion, all of the planned mass spectrometer measurements were acquired. A great deal of data analysis remains along with comparisons to other measurements.^{3,4} In future flights it would be desirable to have many more ram observations spaced properly throughout flight plus the capability of placing the spectrometer on the RMS. Such measurements would be much easier to interpret.

Acknowledgments

The contributions of the following people to the success of the spectrometer experiment are gratefully acknowledged: R.E. McNerny and co-workers, AFGL; R. Wilton and co-workers, AFGL; J. Ballenthin, AFGL; Col. R.B. Kehl, Space Division; C. McDowell, Lockheed Missile and Space Co.; E. Szuszczewicz and J. Holmes, NRL; R. Eng and R. Morin, Northeastern University. This work was funded by the Air Force Office of Scientific Research under Task 2310G3.

References

1. R. Narcisi, E. Trzcinski, G. Federico, L. Wlodyka and D. Delorey, "Shuttle Mass Spectrometer Measurements," Air Force Geophysics Laboratory, Internal Report, June 1983.
2. R.S. Narcisi, "Quantitative Determination of the Outgassing Water Vapor Concentrations Surrounding Space Vehicles From Ion Mass Spectrometer Measurements," Adv. Space Res., Vol. 2, No. 10, pp 283-286, 1983.
3. S.D. Shawhan and G.B. Murphy, "Plasma Diagnostics Package Assessment of the STS-3 Orbit Environment and Systems for Science," presented at the AIAA 21st Aerospace Sciences Meeting, January 10-13, 1982, Reno Nevada, paper AIAA-83-0253.
4. G.R. Carignan and E.R. Miller, "Mass Spectrometer," in STS-2,-3,-4 Induced Environment Contamination Monitor (IECM) Summary Report, E.R. Miller, Editor, NASA TM-82524, February 1983.

Accession For	
NTIS GRA&I	<input checked="" type="checkbox"/>
DTIC TAB	<input type="checkbox"/>
Unannounced	<input type="checkbox"/>
Justification	
By	
Distribution/	
Availability Codes	
Dist	Avail and/or Special
A	SECRET



DTIC
ELECTE
OCT 21 1983

S
D

Unclassified

SECURITY CLASSIFICATION OF THIS PAGE

REPORT DOCUMENTATION PAGE

1a. REPORT SECURITY CLASSIFICATION Unclassified		1b. RESTRICTIVE MARKINGS	
2a. SECURITY CLASSIFICATION AUTHORITY		3. DISTRIBUTION/AVAILABILITY OF REPORT Approved for public release; Distribution unlimited.	
2b. DECLASSIFICATION/DOWNGRADING SCHEDULE		5. MONITORING ORGANIZATION REPORT NUMBER(S)	
4. PERFORMING ORGANIZATION REPORT NUMBER(S) AFGL-TR-83-0261		7a. NAME OF MONITORING ORGANIZATION	
6a. NAME OF PERFORMING ORGANIZATION Air Force Geophysics Laboratory	6b. OFFICE SYMBOL (If applicable) LKD	7b. ADDRESS (City, State and ZIP Code)	
6c. ADDRESS (City, State and ZIP Code) Hanscom AFB, Massachusetts 01731		9. PROCUREMENT INSTRUMENT IDENTIFICATION NUMBER	
8a. NAME OF FUNDING/SPONSORING ORGANIZATION	8b. OFFICE SYMBOL (If applicable)	10. SOURCE OF FUNDING NOS.	
8c. ADDRESS (City, State and ZIP Code)		PROGRAM ELEMENT NO. 61102F	PROJECT NO. 2310
11. TITLE (Include Security Classification) (U) The Gaseous and Plasma Environment Around Space Shuttle		TASK NO. G3	WORK UNIT NO. 09
12. PERSONAL AUTHOR(S) R. Narcisi, E. Trzcinski, G. Federico, L. Wlodyka, D. Delorey*			
13a. TYPE OF REPORT REPRINT	13b. TIME COVERED FROM _____ TO _____	14. DATE OF REPORT (Yr., Mo., Day) 1983 October 13	15. PAGE COUNT 8
16. SUPPLEMENTARY NOTATION *Space Data Analysis Laboratory, Boston College, Chestnut Hill, MA To be presented at the AIAA Meeting, Washington, D.C., 1 November 1983			
17. COSATI CODES		18. SUBJECT TERMS (Continue on reverse if necessary and identify by block number)	
FIELD	GROUP	Shuttle contaminant	
	SUB. GR.	Ionospheric irregularities	
19. ABSTRACT (Continue on reverse if necessary and identify by block number) A multi-mode, fast-sampling, quadrupole mass spectrometer was flown on shuttle. The instrument measured the neutral and positive ion composition and densities as well as the vehicle potential. The spectrometer also was able to distinguish the ambient neutral/ion species from the contaminants by separating them in an energy analysis mode. The plasma measurements showed relatively large amounts of H₂O⁺ and H₃O⁺ ions that were created in the water vapor cloud surrounding the spacecraft. Plasma depletions of about an order of magnitude occurred during VCS firings. Examples of vehicle potential measurements performed by sitting on the O⁺ and also the NO⁺ peak while applying a stepped retarding potential are shown. Neutral species measurements indicated the major contaminants were water vapor and helium. The quantity of water vapor detected versus time correlated directly with the temporal variation of spacecraft temperature. Helium was in excessive amounts throughout the flight. The time dependent characteristics of the backscattered exhaust products from the OMS and VCS firings were accurately measured. The major exhaust products were H₂, H₂O and N₂. The largest return flux came from the VCS's located on the spectrometer pointing side. The concentrations of heavy masses (greater than 50 amu) were small.			
20. DISTRIBUTION/AVAILABILITY OF ABSTRACT UNCLASSIFIED/UNLIMITED <input type="checkbox"/> SAME AS RPT. <input checked="" type="checkbox"/> DTIC USER: <input type="checkbox"/>		21. ABSTRACT SECURITY CLASSIFICATION Unclassified	
22a. NAME OF RESPONSIBLE INDIVIDUAL Diane Corazzini		22b. TELEPHONE NUMBER (Include Area Code) (617) 861-4553	22c. OFFICE SYMBOL AFGL/SULR

END

DATE
FILMED

11 - 83

DTIC